Antiviral Research 108 (2014) 142–147

Contents lists available at ScienceDirect

Antiviral Research

journal homepage: www.elsevier.com/locate/antiviral

PEGylated recombinant human interferon-ω as a long-acting antiviral agent: Structure, antiviral activity and pharmacokinetics

Weili Yu [a,c,1], Changming Yu [b,1], Ling Wu [a,c], Ting Fang [b], Rui Qiu [a], Jinlong Zhang [b], Ting Yu [b], Ling Fu [b], Wei Chen [b,*], Tao Hu [a,*]

[a] National Key Laboratory of Biochemical Engineering, Institute of Process Engineering, Chinese Academy of Sciences, Beijing 100190, China
[b] Beijing Institute of Biotechnology, Beijing 100071, China
[c] University of Chinese Academy of Sciences, Beijing 100190, China

ARTICLE INFO

Article history:
Received 25 March 2014
Revised 28 May 2014
Accepted 5 June 2014
Available online 14 June 2014

Keywords:
Interferon-ω
Antiviral agent
PEGylation
Pharmacokinetics

ABSTRACT

Recombinant human interferon-ω (rhIFN-ω) exhibits a potent antiviral activity. Because of poor pharmacokinetics (PK) of rhIFN-ω, frequent dosing of rhIFN-ω is necessitated to achieve the sustained antiviral efficacy. PEGylation can efficiently improve the PK of rhIFN-ω while substantially decrease its bioactivity. The structure, antiviral activity and PK of the PEGylated rhIFN-ω were measured to establish their relationship with PEGylation sites, polyethylene glycol (PEG) mass and PEG structure. Accordingly, N-terminus and the lysine residues were selected as the PEGylation sites. PEGs with M_w of 20 kDa and 40 kDa were used to investigate the effect of PEG mass. Linear and branched PEGs were used to investigate the effect of PEG structure. PEGylation decreased the antiviral activity of rhIFN-ω and improved its PK. The PEGylation sites determine the bioactivity of the PEGylated rhIFN-ω and the conjugated PEG mass determines the PK. N-terminally PEGylated rhIFN-ω with 40 kDa linear PEG maintains 21.7% of the rhIFN-ω antiviral activity with a half-life of 139.6 h. Thus, N-terminally PEGylated rhIFN-ω with linear 40 kDa PEG is a potential antiviral agent for long-acting treatment of the viral diseases.

1. Introduction

Interferon (IFN) is a family of cytokines that potently elicit an antiviral and anti-tumor state in cells (Julander et al., 2007). IFN-α and IFN-β are currently approved and widely used antiviral agents. In contrast, IFN-ω has 62% amino acid identity with IFN-α and 33% amino acid identity with IFN-β (Capon et al., 1985). Because of different antigenicity and immunogenicity between IFN-ω and IFN-α, IFN-ω is a treatment option for the patients who fail to respond to IFN-α. However, the antiviral potency of IFN-ω is limited by its poor pharmacokinetics (PK) (Buckwold et al., 2006). This necessitates frequent dosing of IFN-ω to achieve the sustained antiviral efficacy for treating chronic viral diseases (e.g., hepatitis C virus (HCV) infection).

PEGylation, covalent conjugation of nontoxic polyethylene glycol (PEG), can improve the plasma half-life of a therapeutic protein (Xue et al., 2013). In addition, PEGylation can decrease the proteolytic sensitivity and immunogenicity of the protein (Xue et al., 2013). However, PEGylation is a double-edged sword and can adversely alter the interaction of the protein and its cellular receptors by sterically shielding of the protein's surface (Greenwald et al., 2003). The bioactivity of the protein was decreased by PEGylation. Thus, PEGylation of IFN-ω represents a great challenge to balance these two opposing effects.

Recently, the PEGylated IFN-α2a (PEGASYS, Roche Inc.) and the PEGylated IFN-α2b (PegIntron, Schering-Plough Inc.) have been approved for treatment of HCV infection. Clinical trial results have shown that the PEGylated IFNs produce sustained viral response superior to their respective standard IFN-α (Lindsay et al., 2001; Zeuzem et al., 2000). PEGASYS contains a branched 40 kDa PEG with a half-life of 96 h and 7% of the IFN-α2a antiviral activity. PegIntron contains a linear 12 kDa PEG with a half-life of 45 h and 28% of the IFN-α2b antiviral activity (Boulestin et al., 2006). These pharmacological properties are influenced by the PEG mass, the PEG structure (linear or branched PEG) and the PEGylation site. High PEG mass (e.g., 40 kDa) tends to render low *in vitro* bioactivity

* Corresponding authors. Address: Beijing Institute of Biotechnology, 20 FengTai Dongdajie Street, Beijing 100071, China. Tel.: +86 10 66948801; fax: +86 10 63815273 (W. Chen). Address: National Key Laboratory of Biochemical Engineering, Institute of Process Engineering, Chinese Academy of Sciences, No. 1 Bei-Er-Tiao Street, Haidian District, Beijing 100190, China. Tel.: +86 10 62555217; fax: +86 10 62551813 (T. Hu).

E-mail addresses: cw789661@yahoo.com (W. Chen), thu@ipe.ac.cn (T. Hu).

[1] The authors contribute equally to this work.

http://dx.doi.org/10.1016/j.antiviral.2014.06.003
0166-3542/

of IFN for its strong steric shielding and prolonged plasma half-life of the protein. As compared with linear PEG, branched PEG with same molecular weight (M_w) shows a stronger steric shielding effect and a higher ability to prolong the plasma half-life of the protein. In addition, PEGylation at or near the receptor binding sites can alter the protein's receptor-binding capability. However, systemic investigations on the relationship of the three factors and the PEGylated IFN-ω have not been carried out yet.

In the present study, PEG aldehyde with M_w of 20 kDa and 40 kDa was used for N-terminal mono-PEGylation (i.e., rhIFN-ω was conjugated with one PEG chain at the N-terminus) of recombinant human IFN-ω (rhIFN-ω) (Fig. 1). Maleimide chemistry was used for random mono-PEGylation of rhIFN-ω, using PEG maleimide with M_w of 20 kDa (P20K-mal) and 40 kDa (P40K-mal) (Fig. 1). The PEG reagents used were linear PEGs, except that P40K-mal was a branched PEG consisting of two 20 kDa PEG chains. Structure, antiviral activity and PK of the PEGylated rhIFN-ω samples were investigated in details.

2. Materials and methods

2.1. Materials

rhIFN-ω was prepared and purified as Li et al. (2011). Linear mPEG propionaldehyde with 20 kDa (P20K-ald), linear mPEG propionaldehyde with 40 kDa (P40K-ald), linear mPEG maleimide with 20 kDa (P20K-mal) and branched mPEG maleimide with 40 kDa (P40K-mal) were purchased from Jenkem Biotech (Beijing, China). Trypsin, sodium cyanoborohydride and 2-iminothiolane (IT) were ordered from Sigma (USA). Interferon (α, β, and ω) receptor 2 (IFNAR2) was purchased from Sino Biological Inc. (Beijing, China).

2.2. Preparation of the PEGylated rhIFN-ω

2.2.1. PEG-ald mediated PEGylation

PEG-ald mediated PEGylation was conducted essentially as Mu et al. (2013). rhIFN-ω (2.2 mg/ml, 0.1 mM) was incubated with 0.4 mM P20K-ald and 0.4 mM P40K-ald in the presence of 8.0 mM sodium cyanoborohydride, respectively. The incubation was carried out in 20 mM NaAc-HAc buffer (pH 5.0) at 4 °C for overnight.

2.2.2. IT-mediated PEGylation

IT-mediated PEGylation was conducted essentially as Liu et al. (2012b). rhIFN-ω (2.2 mg/ml, 0.1 mM) was incubated with 0.4 mM P20K-mal and 0.4 mM P40K-mal in the presence of 0.4 mM IT, respectively. The incubation was carried out in 20 mM sodium phosphate buffer (pH 7.4) at 4 °C for overnight.

2.3. Purification of the PEGylated rhIFN-ω

The reaction mixtures were subjected to an SP Sepharose HP column (1.6 cm × 25 cm, GE Healthcare) for removal of the free PEG reagent. Then, the mixture of rhIFN-ω and the PEGylated rhIFN-ω eluted from the column were loaded on a Superdex 200 column (2.6 cm × 60 cm, GE Healthcare) based on size exclusion chromatography. The fractions corresponding to the PEGylated rhIFN-ω were pooled and concentrated.

2.4. Analytical methods

SEC analysis of the rhIFN-ω samples was carried out as Xue et al. (2013). Bicinchoninic acid protein assay kit (Vigorous Biotechnology, Beijing, China) was used to measure the concentrations of the rhIFN-ω samples. SDS–PAGE analysis was conducted using a 15% polyacrylamide gel. The gel was stained with Coomassie blue R-250.

2.5. Characterization of the sites of PEGylation

Tryptic digestion of the rhIFN-ω samples was performed in 50 mM NH_4HCO_3 containing 2 M urea (pH 8.3) at an enzyme-to-substrate ratio of 1:50 (w/w) at 37 °C for overnight. The resultant tryptic peptides were analyzed as Liu et al. (2012a). Since Arg^{74} and Arg^{123} cannot be modified by PEG, the recovery of peptide T11 (75-123) was used as an internal standard.

2.6. Circular dichroism

The rhIFN-ω samples were analyzed by the far-UV circular dichroism (CD) at 25 °C, using a JASCO J-810 spectropolarimeter (JASCO, Japan) with a 0.1 cm light path cuvette. All the rhIFN-ω samples were at a protein concentration of 0.1 mg/ml in 20 mM sodium phosphate buffer (pH 7.4). The spectra of buffer blanks were measured before the samples and subtracted from the spectra of the samples.

2.7. Sedimentation velocity

Sedimentation velocity measurements were performed by analytical ultracentrifugation on a ProteomeLab XL-1 (Beckman, USA) equipped with an An-60Ti rotor. The sedimentation coefficient (S) and the ratio of frictional coefficient (f/f_0) of the rhIFN-ω samples were determined essentially as Hu et al. (2007).

2.8. Surface plasmon resonance

The binding affinity of the rhIFN-ω samples to IFNAR2 was measured using surface plasmon resonance (SPR) analysis on a BIAcore 3000 instrument (Biacore, Sweden) essentially as Liu et al. (2012a).

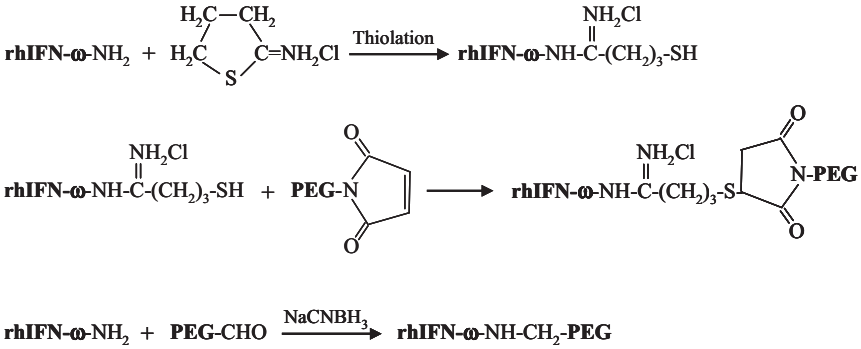

Fig. 1. Schematic representation for preparation of the PEGylated rhIFN-ω.

2.9. Antiviral activity

The antiviral activity was evaluated according to the cell pathogenic effect of vesicular stomatitis virus on WISH cells (Li et al., 2011). The inhibitory effect of rhIFN-ω on the virus induced cell lysis was measured and used for calculating the antiviral activity of the rhIFN-ω samples.

2.10. Pharmacokinetics studies

Twenty-five adult male New Zealand white rabbits weighing 2.3–2.8 kg were used for the pharmacokinetics studies. The study was randomized but not blinded and involved five groups with five rabbits in each. The groups were rhIFN-ω, IFN-ald-P20K, IFN-ald-P40K, IFN-mal-P20K, and IFN-mal-P40K. The rhIFN-ω samples (20 μg protein per kg body weight) were injected subcutaneously.

Blood samples were drawn via the ear vein at 0, 0.1, 0.5, 1, 2, 4, 8, 12, 24, 48, 72, 96, 120, 144, 168, 192, 216, 288 and 312 h after subcutaneous injection of the rhIFN-ω samples. The rhIFN-ω concentrations in plasma were assayed by a human IFN-ω ELISA kit (Bender MedSystems™). Results were expressed as mean values ± SD. Pharmacokinetic parameters, including half-life ($t_{1/2}$), plasma peak concentration (C_{max}), peak retention time (T_{max}), area under the curve (AUC_{0-t}), and clearance over bioavailability (CF) were calculated using a PKsolver 2.0 software.

2.11. Statistical analysis

All statistical analyses were performed using GraphPadPrism 5 software (GraphPad Software, San Diego, CA, USA).

3. Results

3.1. Size exclusion chromatography

Under the present experimental conditions, PEGylation of rhIFN-ω led to a mixture containing approximately 40–45% mono-PEGylated rhIFN-ω, 5–10% highly PEGylated forms and 45–55% unPEGylated rhIFN-ω. The mono-PEGylated forms were separated from the mixtures by an SP Sepharose HP column (1.6 cm × 25 cm) and a Superdex 200 column (2.6 cm × 60 cm).

The purified PEGylated proteins were further analyzed by a Superdex 200 column (1.0 cm × 30 cm). The P20K-ald mediated mono-PEGylated rhIFN-ω (IFN-ald-P20K) and the P20K-mal mediated one (IFN-mal-P20K) were both eluted as symmetric peaks (Fig. 2a). These elution peaks were left-shifted as compared with the one corresponding to rhIFN-ω. This indicated that the hydrodynamic volume of rhIFN-ω was increased by PEGylation. IFN-mal-P20K was eluted slightly earlier than IFN-ald-P20K. This indicated that IFN-mal-P20K showed higher hydrodynamic volume than IFN-ald-P20K. The P40K-ald mediated one (IFN-ald-P40K) and the P40K-mal mediated one (IFN-mal-P40K) were eluted earlier than IFN-mal-P20K. This indicated that 40 kDa PEG can induce higher hydrodynamic volume of rhIFN-ω than 20 kDa PEG.

3.2. SDS–PAGE

The rhIFN-ω samples were analyzed by SDS–PAGE (Fig. 2b). rhIFN-ω showed a single band corresponding to an apparent M_w of 22 kDa (Lane 2). The four PEGylated rhIFN-ω samples all showed a single band, indicating their high purity. IFN-ald-P20K (Lane 3) and IFN-mal-P20K (Lane 5) both showed a single band corresponding to an apparent M_w of ~60 kDa. Moreover, IFN-ald-P40K (Lane 4) and IFN-mal-P40K (Lane 6) both showed a single band corresponding to an apparent M_w of ~110 kDa. The aberrant band migration of the PEGylated products was due to the conjugated PEG that can efficiently bind water molecules.

3.3. Characterization of the PEGylation sites

The sites of PEGylation in IFN-ald-P20K and IFN-mal-P20K were characterized by tryptic peptide mapping. As compared to that of rhIFN-ω, the peak corresponding to the peptide T1 (1–14, LGCDLPQNHGLLSR) was essentially disappeared for IFN-ald-P20K (Fig. 3). In contrast, other tryptic peptides of rhIFN-ω were essentially intact as compared to rhIFN-ω. Since Arg^{14} cannot be modified by PEG, the N-terminus (i.e., Leu^{1}) of rhIFN-ω was specifically PEGylated in IFN-ald-P20K. Similar result was observed for IFN-ald-P40K (data not shown).

As indicated by the asterisks in Fig. 3, the peaks corresponding to the peptides T1, T4 (26–33, ISPFLCLK), T17 + 18 (138–152, YSDCAWEVVRMEIMK) and T14 (131–134, VYLK) for IFN-mal-P20K were decreased as compared to that of rhIFN-ω. This suggested that IFN-mal-P20K consisted of at least four positional isomers, which were mixtures with single PEG chain modified at Leu^{1}, Lys^{33}, Lys^{134} and Lys^{152} of rhIFN-ω. Similar result was observed for IFN-mal-P40K (data not shown).

3.4. Circular dichroism

The secondary structure of the rhIFN-ω samples was investigated by CD spectroscopy. As shown in Fig. 4a and b, the far-UV

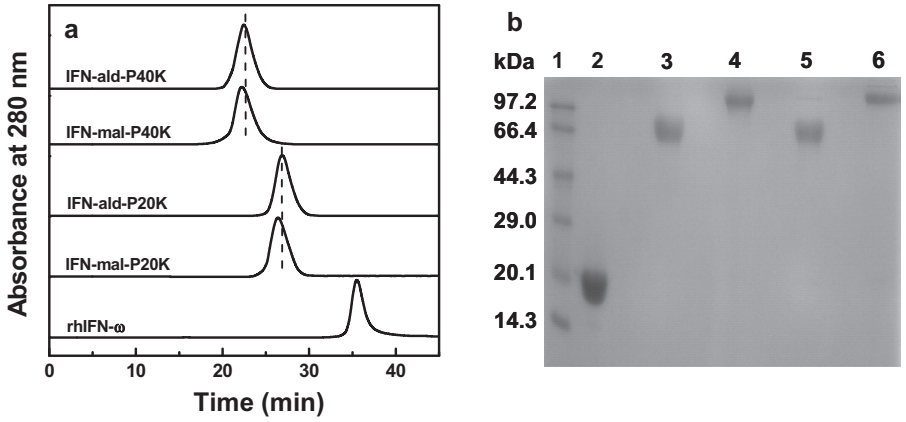

Fig. 2. Characterization of the rhIFN-ω samples. SEC analysis (a) was performed on a Superdex 200 column (1 cm × 30 cm). The column was equilibrated and eluted with 20 mM sodium phosphate (pH 7.4) at a flow rate of 0.5 mL/min. SDS–PAGE analysis (b) was carried out on a 14% Tris–glycine gel. Lane 1, the molecular weight markers; lane 2, rhIFN-ω; lane 3, IFN-ald-P20K; lane 4, IFN-ald-P40K; lane 5, IFN-mal-P20K; and lane 6, IFN-mal-P40K.

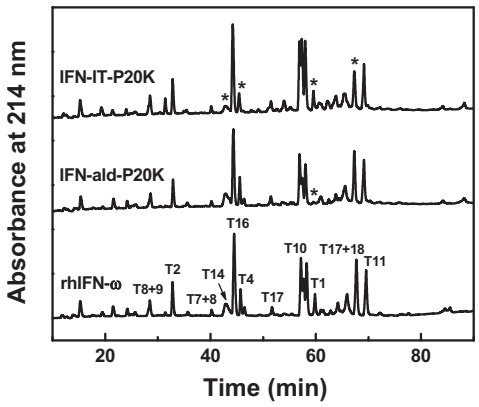

Fig. 3. Tryptic peptide mapping analysis of the sites of PEGlation. The tryptic peptides were analyzed using a Proteonavi column (4.6 mm × 250 mm). The peaks corresponding to the PEGylated peptides were indicated as asterisk. The column was eluted with 5% acetonitrile containing 0.1% trifluoroacetic acid (TFA) for 15 min, followed by elution with a linear gradient of 5–50% acetonitrile containing 0.1% TFA for 100 min at a flow rate of 0.5 ml/min.

CD spectra (200–260 nm) of rhIFN-ω showed a doublet band, indicating the presence of rich α-helix and β-sheet in rhIFN-ω. The CD spectra of the four PEGylated rhIFN-ω samples were essentially superimposed on that of rhIFN-ω. This indicated that PEGylation did not change the overall secondary structure of rhIFN-ω.

3.5. Sedimentation velocity

As shown in Table 1, PEGylation can dramatically decrease the $S^0_{20,W}$ of rhIFN-ω as a function of the conjugated PEG mass. This suggested that PEGylation can dramatically alter the hydrodynamic behaviors of rhIFN-ω. IFN-mal-P20K showed a lower $S^0_{20,W}$ than IFN-ald-P20K, due to the larger hydrodynamic volume of IFN-mal-P20K. IFN-mal-P40K showed a lower $S^0_{20,W}$ than IFN-ald-P40K, indicating that PEG branching can lead to compact conformation of PEG.

The ratio of frictional coefficient (f/f_0) was used to provide hydrodynamic shape of rhIFN-ω. As reflected by the increased f/f_0, the overall shape of the PEGylated rhIFN-ω became highly asymmetric (Table 1). IFN-ald-P20K showed an f/f_0 lower than IFN-mal-P20K. However, the f/f_0 of IFN-ald-P40K was comparable to IFN-mal-P40K. Thus, the branched PEG (i.e., two PEG chains branched at one site) can decrease the molecular shape asymmetry of the PEGylated rhIFN-ω, reflecting a strong steric shielding effect of the branched PEG on rhIFN-ω.

3.6. Surface plasmon resonance

SPR analysis was conducted to investigate the interaction between the rhIFN-ω samples and their receptor (IFNAR2). The association rate (k_a), dissociation rate (k_d), and dissociation constant (K_D) were summarized in Table 2. The k_d values of the four PEGylated rhIFN-ω samples were slightly increased as compared with that of rhIFN-ω. This indicated that PEGylation slightly decreased the dissociation of the rhIFN-ω/IFNAR2 complex. In contrast, PEGylation of rhIFN-ω led to a decrease in the k_a and an increase in the K_D. As compared with IFN-ald-P20K, IFN-mal-P20K showed 1.25-fold increase in the K_D. This was due to that the N-terminus was far from the receptor binding site of rhIFN-ω. Thus, N-terminal PEGylation can decrease the loss of antiviral activity of rhIFN-ω. In addition, IFN-mal-P40K showed 2.47-fold increase in the K_D as compared with IFN-ald-P40K. This indicated that the modification sites can determine the interaction between IFNAR2 and rhIFN-ω and significantly influence the bioactivity of the PEGylated rhIFN-ω.

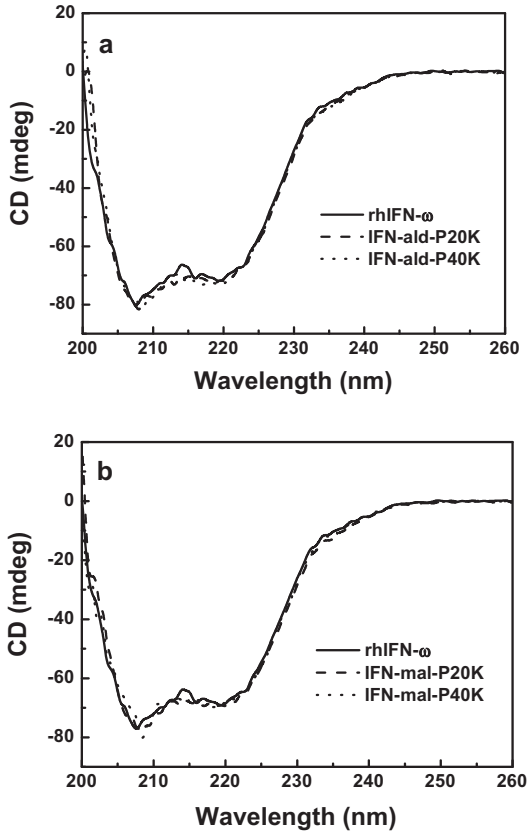

Fig. 4. Circular dichroism analysis of the rhIFN-ω samples. The spectra of IFN-ald-PEG (a) and IFN-mal-PEG (b) were recorded in the range of 200–260 nm.

Table 1
Sedimentation velocity analysis of the rhIFN-ω samples.

Sample	$S^0_{20,w}$ [a]	f/f_0 [b]
rhIFN-ω	2.17 ± 0.12	1.29
IFN-ald-P20K	1.34 ± 0.05	2.74
IFN-mal-P20K	1.23 ± 0.05	2.99
IFN-ald-P40K	0.95 ± 0.05	4.77
IFN-mal-P40K	0.82 ± 0.04	4.74

[a] The sedimentation coefficient.
[b] The ratio of frictional coefficient.

Table 2
Surface plasmon resonance analysis of the rhIFN-ω samples.

Sample	k_a (10^5 M^{-1} s^{-1})[a]	k_d (10^{-3} s^{-1})[b]	K_D (10^{-9} M)[c]
rhIFN-ω	9.23	4.30	4.7
IFN-ald-P20K	3.16	6.94	22.0
IFN-mal-P20K	2.70	7.40	27.4
IFN-ald-P40K	2.01	6.47	32.2
IFN-mal-P40K	0.73	5.81	79.6

[a] The association rate.
[b] The dissociation rate.
[c] The dissociation constant that is equal to k_d/k_a.

3.7. Antiviral activity

As shown in Table 3, the antiviral activities of the four PEGylated rhIFN-ω samples were lower than that of rhIFN-ω. IFN-mal-P20K showed a lower antiviral activity than IFN-ald-P20K, consistent with the SPR results. This was due to that some PEGylated lysine residues in IFN-mal-P20K were proximal to the

receptor binding sites. Moreover, IFN-mal-P40K showed a much lower antiviral activity than IFN-ald-P40K. This further confirmed that the modification sites can significantly influence the antiviral activity of the PEGylated rhIFN-ω.

3.8. Pharmacokinetics

As shown in Fig. 5 and Table 4, rhIFN-ω was rapidly cleared from the plasma after administration with a plasma half-life ($t_{1/2}$) of 1.54 h. As compared with rhIFN-ω, IFN-ald-P20K, IFN-mal-P20K, IFN-ald-P40K and IFN-mal-P40K showed 26.3-, 27.1-, 90.6- and 84.7-fold increase in the $t_{1/2}$, respectively. The four PEGylated rhIFN-ω samples also displayed 67.0-, 61.0-, 167.0- and 147.7-fold decrease in the CL. This revealed markedly prolonged serum presence of rhIFN-ω by PEGylation. In addition, IFN-ald-P40K showed slightly higher $t_{1/2}$ and lower CL than IFN-mal-P40K. rhIFN-ω was absorbed with T_{max} of 0.5 h, followed by rapid decline in serum. In contrast, IFN-ald-P20K, IFN-mal-P20K, IFN-ald-P40K and IFN-mal-P40K were more slowly absorbed with T_{max} of 4.0–8.0 h and showed an increase in C_{max}. The four PEGylated rhIFN-ω samples displayed 17.8-, 16.3-, 31.8- and 29.8-fold increase in AUC, respectively. Thus, PEGylation can markedly increase the PK of rhIFN-ω as a function of PEG mass. In addition, the PEGylation site and PEG structure did not significantly alter the PK properties of rhIFN-ω.

Table 3
Antiviral activity of the rhIFN-ω samples.

Sample	Antiviral activity [a] (10^6 IU mg^{-1})	Residual activity (%)
rhIFN-ω	83.0	100
IFN-ald-P20K	35.0	42.2
IFN-mal-P20K	22.8	27.5
IFN-ald-P40K	18.0	21.7
IFN-mal-P40K	8.5	10.2

[a] The antiviral activity was assayed according to the cell pathogenic effect (CPE) of vesicular stomatitis virus (VSV) on WISH cells.

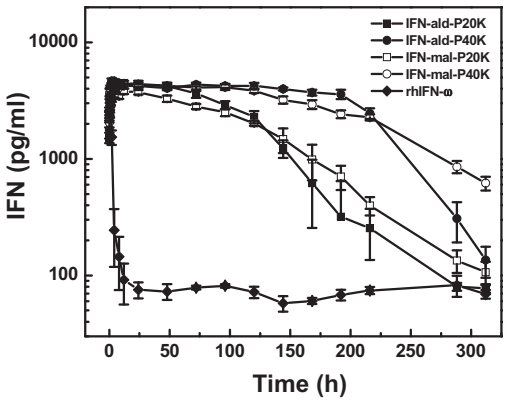

Fig. 5. Blood clearance of the rhIFN-ω samples in New Zealand white rabbits following a single subcutaneous injection. The measurement was carried out using ELISA and each sample was measured for three times.

4. Discussion

The present study focused on development of a long-acting antiviral agent through PEGylation of rhIFN-ω. IFN-ω diverged from IFN-α/β and has biological properties similar to IFN-α/β. These IFNs have been approved to treat chronic hepatitis B, chronic hepatitis C and AIDs-related Kaposi's Sarcoma (Bekisz et al., 2004). IFN-ω was also found as a potent antiviral agent against H1N1 influenza virus, bovine viral diarrhea virus, yellow fever virus and West Nile virus (Buckwold et al., 2007; Xu et al., 2011). In addition, the protective response against two emerging arthropod-borne viral pathogens, dengue virus and chikungunya virus were largely independent of the type I IFN response (Olagnier et al., 2014).

PEGylation decreased the antiviral activity of IFN and prolonged the plasma half-life of IFN. The long *in vivo* presence of IFN can compensate the loss in the antiviral activity of IFN. Thus, the PEGylated IFN is currently used as a long-acting antiviral agent to treat chronic viral disease such as HCV, due to the long treatment period for chronic viral disease (Zeuzem et al., 2000). Treatment of emerging viral diseases with the PEGylated rhIFN-ω should be of great interest, although the treatment may be challenged for its low *in vitro* antiviral activity.

The large number of hydrogen atoms along the PEG chain allowed for extensive hydrogen bonding with water molecules, which can significantly increase the hydrodynamic volume of rhIFN-ω. However, the bulky PEG can sterically shield the receptor binding sites of rhIFN-ω and decrease the antiviral activity of rhIFN-ω. Moreover, the PEGylation sites were important to maintain the antiviral activity of rhIFN-ω. N-terminus (Leu^1) was far from the receptor binding sites of rhIFN-ω. In contrast, Lys^{134} and Lys^{152} were proximal to the receptor binding sites of rhIFN-ω. Thus, IFN-ald-P40K maintained 21.7% of the rhIFN-ω antiviral activity, which was higher than IFN-mal-P40K (10.2%) and PEGASYS that maintained 7% of the IFN-α2a antiviral activity (Boulestin et al., 2006). PEGylation can significantly improve the PK of rhIFN-ω, as reflected by the $t_{1/2}$ values of IFN-ald-P40K (139.6 h) and IFN-mal-P40K (130.4 h) that are higher than the one of PEGASYS (~96 h).

In summary, high PEG mass can efficiently improve the hydrodynamic volume and PK of rhIFN-ω, whereas it significantly decreased the antiviral activity of rhIFN-ω. N-terminal PEGylation showed higher ability than the random PEGylation to maintain the antiviral activity of rhIFN-ω. The PEGylation sites determine the bioactivity of the PEGylated rhIFN-ω and the conjugated PEG mass

Table 4
Pharmacokinetic parameters of the rhIFN-ω samples.

Sample	C_{max} [a] (pg ml^{-1})	T_{max} [b] (h)	$t_{1/2}$ [c] (h)	CL[d] (ml h^{-1} kg^{-1})	AUC_{0-312h} [e] (pg h ml^{-1})
rhIFN-ω	3241.4	0.5	1.54	101.9	30283
IFN-ald-P20K	4468.6	4.0	40.54	1.52	539011
IFN-mal-P20K	3990.5	4.0	41.71	1.67	493139
IFN-ald-P40K	4660.0	4.0	139.6	0.61	963089
IFN-mal-P40K	4402.4	8.0	130.4	0.69	901727

[a] Plasma peak concentration.
[b] Peak retention time.
[c] Elimination half-life.
[d] Clearance over bioavailability.
[e] Area under drug concentration versus time curve.

determines the PK. Thus, N-terminally PEGylated rhIFN-ω with linear 40 kDa PEG is a potential antiviral agent for long-acting treatment of antiviral disease.

Acknowledgments

This study was financially supported by Natural Science Foundation of China (20906095), Beijing Natural Science Foundation (7142104) and Hundred Talents Program of Chinese Academy of Sciences.

References

Bekisz, J., Schmeisser, H., Hernandez, J., Goldman, N.D., Zoon, K.C., 2004. Human interferons alpha, beta and omega. Growth Factors 22, 243–251.

Boulestin, A., Kamar, N., Sandres-Saune, K., Alric, L., Vinel, J.P., Rostaing, L., Izopet, J., 2006. Pegylation of IFN-α and antiviral activity. J. Interfer. Cytokine Res. 26, 849–853.

Buckwold, V.E., Lang, W., Scribner, C., Blanchett, D., Alessi, T., Langecker, P., 2006. Safety pharmacology, toxicology and pharmacokinetic assessment of recombinant human ω-interferon produced from CHO-SS cells. Basic Clin. Pharmacol. Toxicol. 99, 62–70.

Buckwold, V.E., Wei, J., Huang, Z., Huang, C., Nalca, A., Wells, J., Russell, J., Collins, B., Ptak, R., Lang, W., Scribner, C., Blanchett, D., Alessi, T., Langecker, P., 2007. Antiviral activity of CHO-SS cell-derived human omega interferon and other human interferons against HCV RNA replicons and related viruses. Antiviral Res. 73, 118–125.

Capon, D.J., Shepard, H.M., Goeddel, D.V., 1985. Two distinct families of human and bovine interferon-α genes are coordinately expressed and encode functional polypeptides. Mol. Cell Biol. 5, 768–779.

Greenwald, R.B., Choe, Y.H., McGuire, J., Conover, C.D., 2003. Effective drug delivery by PEGylated drug conjugates. Adv. Drug Del. Rev. 55, 217–250.

Hu, T., Manjula, B.N., Li, D., Brenowitz, M., Acharya, S.A., 2007. Influence of intramolecular cross-links on the molecular, structural and functional properties of PEGylated hemoglobin. Biochem. J. 402, 143–151.

Julander, J.G., Morrey, J.D., Blatt, L.M., Shafer, K., Sidwell, R.W., 2007. Comparison of the inhibitory effects of interferon alfacon-1 and ribavirin on yellow fever virus infection in a hamster model. Antiviral Res. 73, 140–146.

Li, J., Li, B., Zhang, J., Hou, L., Yu, C., Fu, L., Song, X., Yu, T., Zhang, J., Ren, J., Xu, C., Chen, W., 2011. Preparation of CHO cell-derived rhIFN-ω-Fc with improved pharmacokinetics. Antiviral Res. 89, 199–203.

Lindsay, K.L., Trepo, C., Heintges, T., Shiffman, M.L., Gordon, S.C., Hoefs, J.C., Schiff, E.R., Goodman, Z.D., Laughlin, M., Yao, R., Albrecht, J.K., 2001. A randomized, double-blind trial comparing pegylated interferon alfa-2b to interferon alfa-2b as initial treatment for chronic hepatitis C. Hepatology 34, 395–403.

Liu, R., Li, D., Wang, J., Qiu, R., Lin, Q., Zhang, G., Ma, G., Su, Z., Hu, T., 2012a. Preparation, characterization and in vitro bioactivity of N-terminally PEGylated staphylokinase dimers. Process Biochem. 47, 41–46.

Liu, S., Sun, L., Wang, J., Ma, G., Su, Z., Hu, T., 2012b. Mono-PEGylation of ribonuclease A: high PEGylation efficiency by thiolation with small molecular weight reagent. Process Biochem. 47, 1364–1370.

Mu, Q., Hu, T., Yu, J., 2013. Molecular insight into the steric shielding effect of PEG on the conjugated staphylokinase: biochemical characterization and molecular dynamics simulation. PLoS One 8, e68559.

Olagnier, D., Scholte, F.E.M., Chiang, C., Albulescu, I.C., Nichols, C., He, Z., Lin, R., Snijder, E.J., van Hemert, M.J., Hiscotta, J., 2014. Inhibition of dengue and chikungunya virus infections by RIG-I-mediated type I interferon-independent stimulation of the innate antiviral response. J. Virol. 88, 4180–4194.

Xu, C., Song, X., Fu, L., Dong, D., Wu, S., Li, G., Yi, S., Yu, T., Yu, R., Hou, L., Chen, W., 2011. Antiviral potential of exogenous human omega interferon to inhibit pandemic 2009A (H1N1) Influenza virus. Viral Immunol. 24, 369–374.

Xue, X., Li, D., Yu, J., Ma, G., Su, Z., Hu, T., 2013. Phenyl linker-induced dense PEG conformation improves the efficacy of C-terminally mono-PEGylated staphylokinase. Biomacromolecules 14, 331–341.

Zeuzem, S., Feinman, S.V., Rasenack, J., Heathcote, E.J., Lai, M.Y., Gane, E., O'Grady, J., Reichen, J., Diago, M., Lin, A., Hoffman, J., Brunda, M.J., 2000. Peginterferon alfa-2a in patients with chronic hepatitis C. N. Engl. J. Med. 343, 1666–1672.